

POTENTIAL STRUCTURAL TRAPS ASSOCIATED WITH LOWER CARBONIFEROUS SALT IN THE NORTHERN TARIM BASIN, NW CHINA

Jiangyu Zhou^{*#}, Zhongmin Lin^{**}, Chuangrong Luo^{***}
and Xiepei Wang[#]

In the Aixieke-Santamu area of the northern Tarim Basin (NW China), 45 relatively low amplitude structures related to the plastic flow of Lower Carboniferous salt have been discovered in the Lower Carboniferous Kalashayi Formation and the Middle-Upper Triassic Akekule and Halahatan Formations. Three small hydrocarbon accumulations have so far been located at the margins of a Lower Carboniferous salt body (measuring about 55km × 75km and 115-225m thick, controlled by wells and 2D and 3D seismic sections). In this paper, we consider the development of this salt body and discuss possible reasons why vertical diapirs are absent from the study area. We attempt to develop a model of salt flow and we investigate the relationship between salt flow and the occurrence of oil and gas traps.

Using recently-acquired high-resolution 2D and 3D seismic profiles, we show that the Lower Carboniferous salt has undergone three separate phases of plastic flow. At the end of the Early Permian, the salt flowed southwards by 2.0-2.8 km; then, during the Late Triassic — Early Jurassic, it flowed in the same direction by 1.0-1.8 km; and finally at the end of the Tertiary, it flowed northwards by 0.6-1.5 km. These movements resulted in the formation of various types of structural trap in the Kalashayi, Akekule and Halahatan Formations including salt ridge anticlines, domes and marginal troughs. Salt ridge and salt edge low-amplitude anticlines are probably the most important targets for future hydrocarbon exploration.

INTRODUCTION

Interest in the northern Tarim Basin (NW China) has recently increased following the discovery of oil and gas traps related to the flow of Lower Carboniferous salt. Traps related to salt migration constitute major plays in many parts of the World including the US Mississippi salt basin and the Southern North Sea

(Jenyon, 1986, 1988; Jackson *et al.*, 1989; Montgomery *et al.*, 1997). The plastic deformation of salt can give rise to a range of features including folds, faults and collapse structures (Jenyon, 1986, 1988; Wu *et al.*, 1990; Nelson, 1991; Seni, 1992; Jackson, 1995; Rowan *et al.*, 1995, 1999). The growth of subsalt and suprasalt structures can be triggered by a number of mechanisms, among which the role of regional extension has been emphasized (Jackson *et al.*, 1994; Rowan *et al.*, 1995; Schultz-Ela *et al.*, 1996). Differential depositional loading can induce the flow of salt and trigger diapirism (Koyi *et al.*, 1993; Jackson, 1995). The effects of aggradation and progradation on salt sheet emplacement and segmentation have also been discussed (Koyi, 1996; Ge *et al.*, 1997). Scaled physical models (West, 1989; Koyi *et al.*, 1993; Letouzey *et al.*, 1995; Ge *et al.*, 1997) have been used to study processes of salt deformation and the evolution of salt-related structures in different geological settings. With the development of 3D seismic and computer modelling techniques, it

* Guangzhou Institute of Geochemistry, Chinese Academy of Sciences, PO Box 1131, Wushan, Guangzhou 510640, P. R. China.

** Northwest Bureau of Petroleum Geology, CINOPEC, Urumqi 83001, P. R. China.

*** Research Institute of Petroleum Exploration, CINOPEC, Jingzhou, Hubei 434100, P. R. China.

Present address: Faculty of Earth Resources, China University of Geosciences, Wuhan 430074, P. R. China.

Author for correspondence, email: zjy522@cug.edu.cn

System (seismic reflection boundary)	Series	Formation	Symbol	Member	Thickness (m)	Source	Oil Reservoir	Seal
Triassic (T05)	Upper	Halahatan	T3h	Mudstone	60-70			
				Sandstone	80-90			
	Middle	Akekule	T2a	Upper Mudstone	49-57			
				Upper Sandstone	26-34			
				Lower Mudstone	20-30			
				Lower Sandstone	120-140			
	Lower	Ketuer	T1k	Mudstone	50-80			
Carboni- ferous (T06)	Upper	Xiaohaizi	C2x	Limestone	40-136			
	Lower	Kalashayi	C1kl	Sandstone - Mudstone	192-577			
				Upper Mudstone	40-117			
		Bachu	C1b	Double-peak limestone	15-25			
				Gypsum- halite	115-225			
				Lower Mudstone	40-60			
	Sandstones - Congloms.	0-90						

Table 1. Generalized stratigraphic column for the Akekule area in the northern Tarim Basin.

is now possible to analyze physical models simulating salt deformation processes and salt structures in a range of geological settings (Koyi, 1992; Guglielmo *et al.*, 1997). There has also been much work on the restoration of salt features and sub- and suprasalt structures related to salt flow using high-resolution seismic data (Jenyon, 1988; Rowan, 1993; Koyi *et al.*, 1993; Montgomery *et al.*, 1997; Rowan *et al.*, 1999).

In this paper, we present 2D and 3D seismic profiles from the northern Tarim Basin which illustrate the occurrence of a variety of salt features. We discuss the characteristics of salt deformation including timing, amplitude, direction and distance of salt migration, and describe a model of salt flow and the evolution of salt-related structures between the Early Carboniferous and the Late Tertiary.

Finally, we comment on (and suggest reasons for) the absence of salt diapirs in the study area.

Geological and stratigraphic setting

The study area is located some 50km south of Luntai in the north of the Tarim Basin, NW China (Fig.1). Throughout much of the Palaeozoic, the roughly east-west trending Shaya-Luntai fault divided an uplifted area to the north from a generally subsiding area to the south (Fig. 1) (Jia, 1999, 2002; Kang, 1996). In the Early Ordovician, carbonates were deposited in semi-restricted to restricted marine settings to the south of the fault and have a present-day thickness of 500-1,000m. They are overlain by Middle-Late Ordovician shallow-water and continental deposits. The Ordovician succession was uplifted and intensely eroded in the Silurian and Devonian (Jia, 1991; Jia *et al.*, 2002; Kang, 1996). During the Carboniferous, the northern Tarim Basin was characterized by coastal tidal flats and evaporative lagoons with an arid climate (Zhou *et al.*, 1999; Gu, 1996); a schematic depositional model is illustrated in Fig. 2.

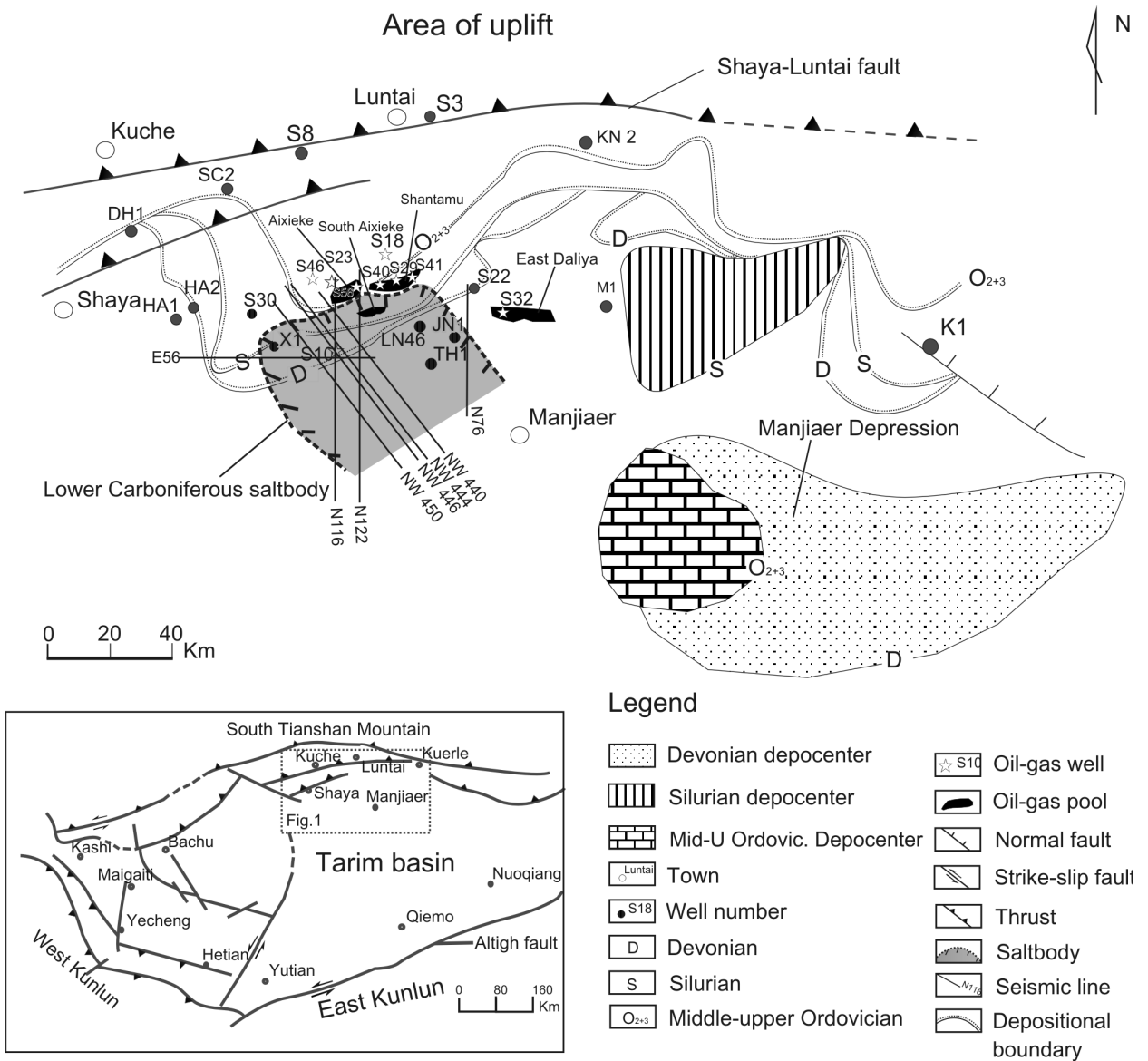


Fig. 1. Schematic map of the northern Tarim Basin (NW China), showing the location of the study area and the saltbody investigated. Also located are the profiles of seismic lines and well locations, together with pre-Carboniferous depocentres and depositional boundaries. Inset shows the regional location of the study area.

The Lower Carboniferous salt-bearing interval, which is the focus of this study, rests unconformably on the Early Palaeozoic and comprises an evaporite succession (halite, gypsum) which is 115-225m thick together with sandstones, mudstones and limestones. The Lower Carboniferous interval consists of the (basal) Bachu, Kalashayi and (uppermost) Xiaohaizi Formations (Table 1). Most of the evaporite intervals are present in the Bachu Formation which, on the basis of core and wireline log data, can be divided into four members (Figs. 3 and 4):

i. The *Basal Sandstone-Conglomerate Member* (up to 90m thick) consists of fine-grained sandstones, pebbly sandstones and conglomerates with interbedded mudstones and siltstones;

ii. The *Mudstone Member* consists of massive mudstones with thin intervals of gypsum, siltstone and sandstone (40-60m thick);

iii. The *Gypsum-Halite Member* (115-225m thick), which comprises halite, gypsum and thin mudstones and siltstones (Table 2);

iv. The so-called “*Double-peak*” *Limestone Member* (15 to 37m thick), consisting of micritic limestones, interbedded with gypsum-siltstone, gypsum mudstone and mudstones. The upper boundary of this member is marked by the T_6^5 seismic horizon, above which rest the mudstones of the Kalashayi Formation (Fig. 3).

Wells	Total thickness (m)	Max. thickness of single bed (m)	Salt bed number	Interbedded lithology
<i>X1</i>	165.3	5.7	13	Mudstone, Siltstone, Muddy-siltstone
<i>S10</i>	225	28	10	Mudstone, Muddy-siltstone
<i>Th1</i>	188.5	23.2	8	Mudstone, Muddy-siltstone
<i>Jn1</i>	115.6	6.5	14	Sandstone, Siltstone, Muddy-siltstone
<i>Ha1</i>	125.4	8.4	6	Siltstone, Muddy-siltstone
<i>Ha2</i>	140.8	10.2	7	Siltstone, Muddy-siltstone
<i>S50</i>	170.2	16.8	9	Mudstone, Muddy-siltstone
<i>Ln45</i>	125.6	6.7	13	Sandstone, Siltstone, Muddy-siltstone
<i>Ln46</i>	138.4	14.3	12	Mudstone, Muddy-siltstone

Table 2. The thickness of the Lower Carboniferous salt-bearing interval at wells in the northern Tarim Basin.

Source and reservoir rocks

Four source rock intervals have been identified in the Tarim Basin (Graham *et al.*, 1990; Kang, 1996; Jia, 1999; Liu Dameng *et al.*, 2003). The oldest of these are Cambrian-Lower Ordovician sapropelic marine carbonates and mudstones in the Manjiaer Depression to the SE of the study area, which generate gas. The most important oil source rocks are Middle-Upper Ordovician sapropelic and mixed marine mudstones occurring in the centre and west of the Manjiaer Depression. The other two source rock intervals (Table 1) are Lower Carboniferous paralic mudstones, and Triassic lacustrine-deltaic mudstones and coals, both of which are widespread in the northern Tarim Basin.

Commercial hydrocarbon accumulations have been discovered in six intervals between the Cambrian and the Eocene. Of these, the most important are (Kang, 1996; Jia *et al.*, 2002): Ordovician fractured and karstified carbonates; Carboniferous shallow-marine sandstones; and Triassic-Jurassic, Upper Cretaceous and Lower Tertiary sandstones.

Reservoir rocks associated with salt migration comprise Carboniferous and Triassic-Lower Jurassic sandstones (Table 1). Based on regional geological data (Zhou *et al.*, 1999; Gu, 1996) together with data from wells and seismic profiles, the Carboniferous salt-bearing interval is interpreted to have been deposited in coastal tidal flats and evaporative lagoons

(Fig. 2), and Carboniferous reservoir rocks consist of tidal-flat and tidal-channel sandstones. Tidal-flat sandstones are generally characterised by sheet-like beds, 0.2-2.0m thick, interbedded with mudstones containing tidal and lenticular bedding and ripple cross-lamination. Other sandbodies have an amalgamated multilateral architecture, a flat top and a convex (scoured) bottom surface, and are composed of fining-upwards sandstones with bidirectional and ripple cross-bedding, flaser and lenticular bedding; they are interpreted as tidal channel-fill deposits (Fig. 5a, 5c, 5e; Fig. 7a,b,c).

These sandstones commonly occur near the T_5^0 seismic horizon in the sag belt at the margins of the studied saltbody, which formed due to material loss as a result of the plastic flow of salt (see below). Some lenticular sandstones, which cannot clearly be recognized from 2D seismic sections, appear to occur above the saltbody (on top of the T_5^0 seismic horizon), or near the T_5^6 and T_5^7 horizons at the top of the saltbody. These sandbodies can clearly be recognized on 3D seismic sections which show that they characteristically appear to have convex top and bottom surfaces. It is also possible that the tidal-flat sandbodies reflect late-stage differential compaction (Fig. 5d, Fig. 9).

Triassic—Lower Jurassic reservoir rocks consist of braid-delta sandstones and are divided into lower, middle

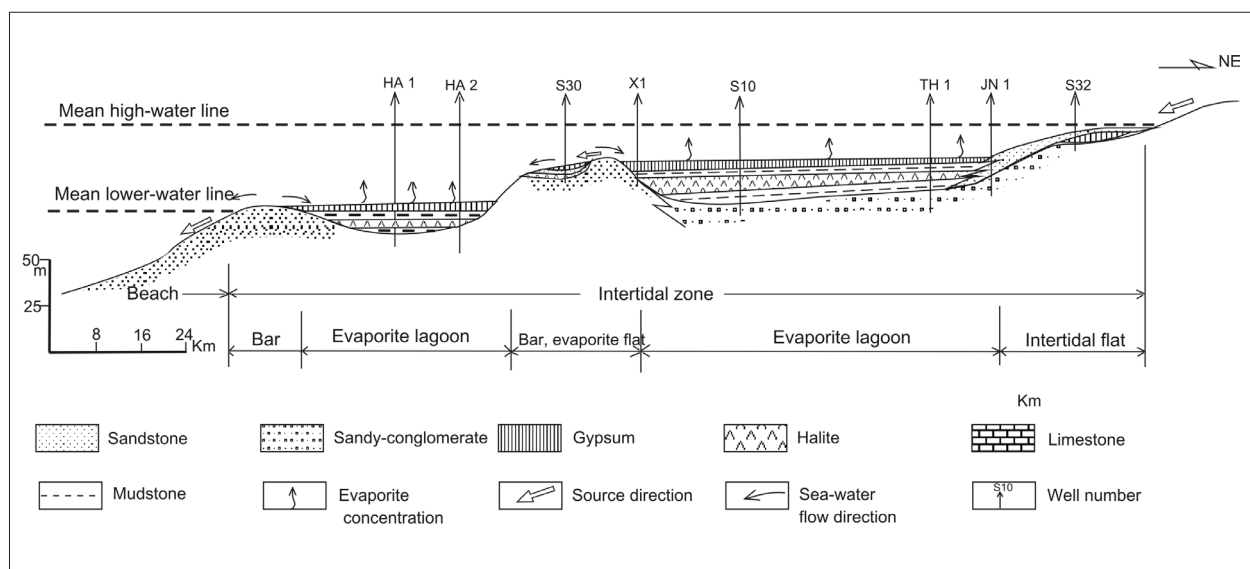


Fig. 2. Schematic depositional model for Lower Carboniferous evaporites and associated deposits in the northern Tarim Basin (after Zhou et al., 1999). For section location, see Fig. 6 (page 77).

and upper groups with thicknesses of 30-80m, 20-40m and 80-150m, respectively (Gu, 1996; Kang, 1996).

MATERIALS AND METHODS

This study uses data from 18 wells located within and close to a Lower Carboniferous saltbody (measuring about 55km×75km), located some 50km south of Luntai in the northern Tarim Basin (Fig. 1). Key wells studied are *Ha1*, *Ha2*, *S30*, *X1*, *S10*, *Th1*, *Jn1*, *S40* and *S32* (see Fig. 1) for which cores together with wireline logs (including spontaneous potential (SP), gamma ray (GR), resistivity (laterolog-8-RILD) and deep investigation induction (RFOC)) were available.

We have interpreted fifteen 2D and five 3D seismic sections across the Lower Carboniferous saltbody including lines *E56*, *N76*, *N116*, *N122*, *NW444*, *NW446* and *NW450* (profile locations in Fig. 1). Examples of these seismic sections are given in Figs. 5a-e with schematic interpretations in Fig. 7.

Wells and 2D seismic sections were used to interpret the thickness of the saltbody and to identify its northern margin together with local structures formed due to salt flow. The upper and lower surfaces of the saltbody, together with salt edge sags and associated faults, were interpreted on 3D sections.

The seismic database consisted of time-migrated sections acquired from the NW Bureau of Petroleum Geology, CINOPEC, with 3D seismic profiles provided by the Nanjing Geophysical Institute and NW Bureau of Petroleum Geology (CNSPC). Seismic lines were mainly orientated NW-SE with a few east-west and south-north strike lines, giving a line spacing varying from 25 to 50m for 3D lines and from 2 to

4km for 2D lines. Data quality is generally good down to 4.0sec and is of high quality within the Lower Carboniferous interval (3.0 to 3.5sec).

GEOLOGY OF SALT STRUCTURES

In this study, we focus on a saltbody located NW of Manjiaer (Fig. 1) which takes the form of a wide, flat sheet measuring about 55km × 75km in plan view. On seismic sections (Fig. 5), the saltbody can be seen to have a flat base; its western and northern margins appear to be well-defined pinch-outs, while the eastern margin is characterized by a facies change to sandstones and mudstones (Fig. 2). Data from wells and seismic sections indicate that the Gypsum-Halite Member of the Bachu Formation is 115m to 225m thick (about 160m on average); maximum thicknesses occur around well *S10* (Table 2). The average thickness of pure gypsum beds is about 120m, and individual beds are up to 28m thick.

An interpretation of 2D and 3D seismic data indicates that deformation of this saltbody was characterized by plastic movement of the western and northern margins but relatively little movement in the east (Fig. 6). Salt migration resulted in the formation of salt ridges and low-amplitude pillows as well as large-scale anticlines. However, vertical and diapiric structures are notable by their absence (Fig. 5).

Timing of Salt Deformation

From the fifteen high-resolution 2D and five 3D seismic profiles available, we have interpreted sag belts of three different ages at the margins of the saltbody; these are filled with tidal-flat or tidal-channel

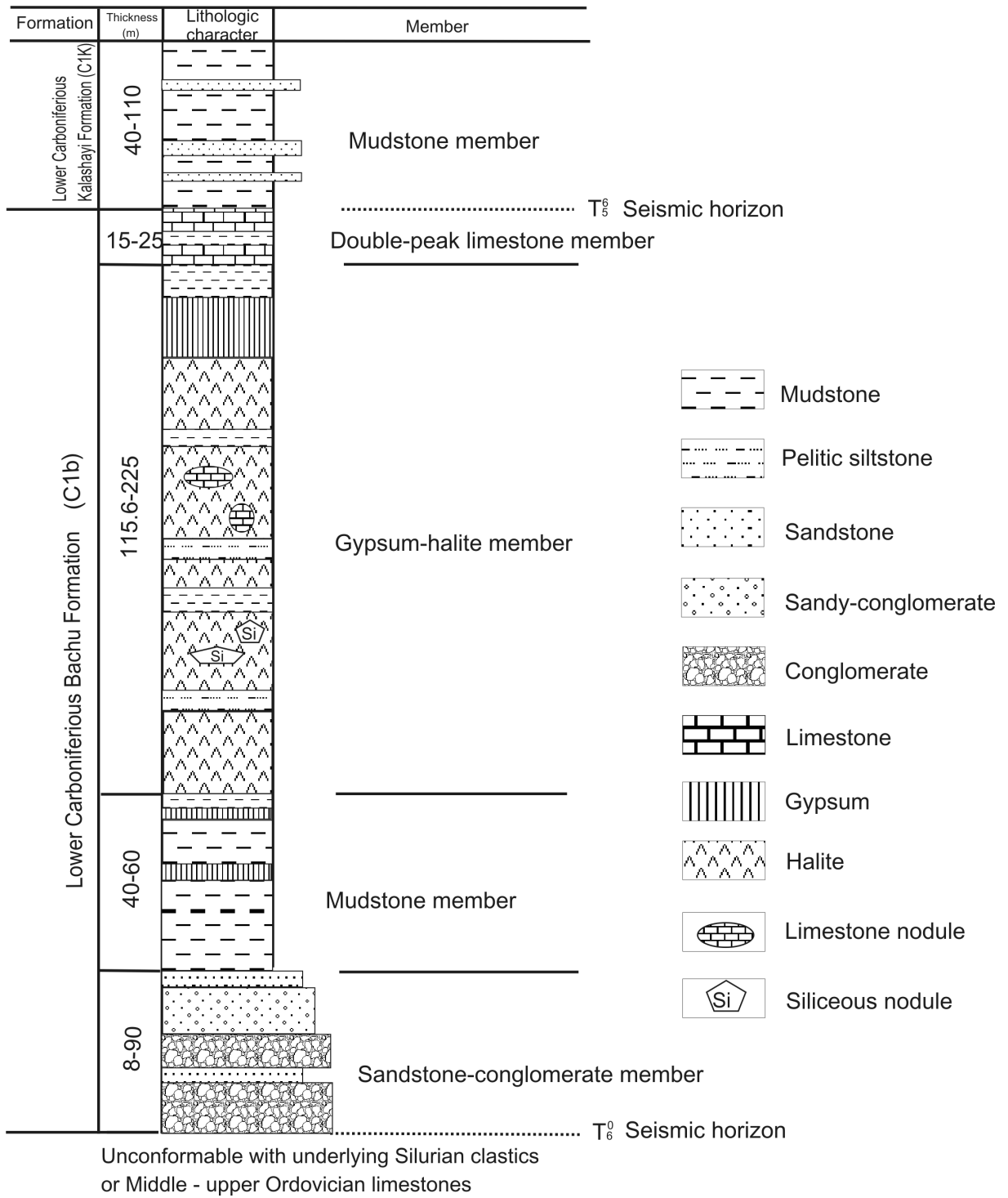


Fig. 3. Generalized lithostratigraphy of the Lower Carboniferous Bachu Formation in the northern Tarim Basin, based on data from wells XI, S10, TH1, JN1, S32, Ln46 and Hal (well locations in Fig. 1).

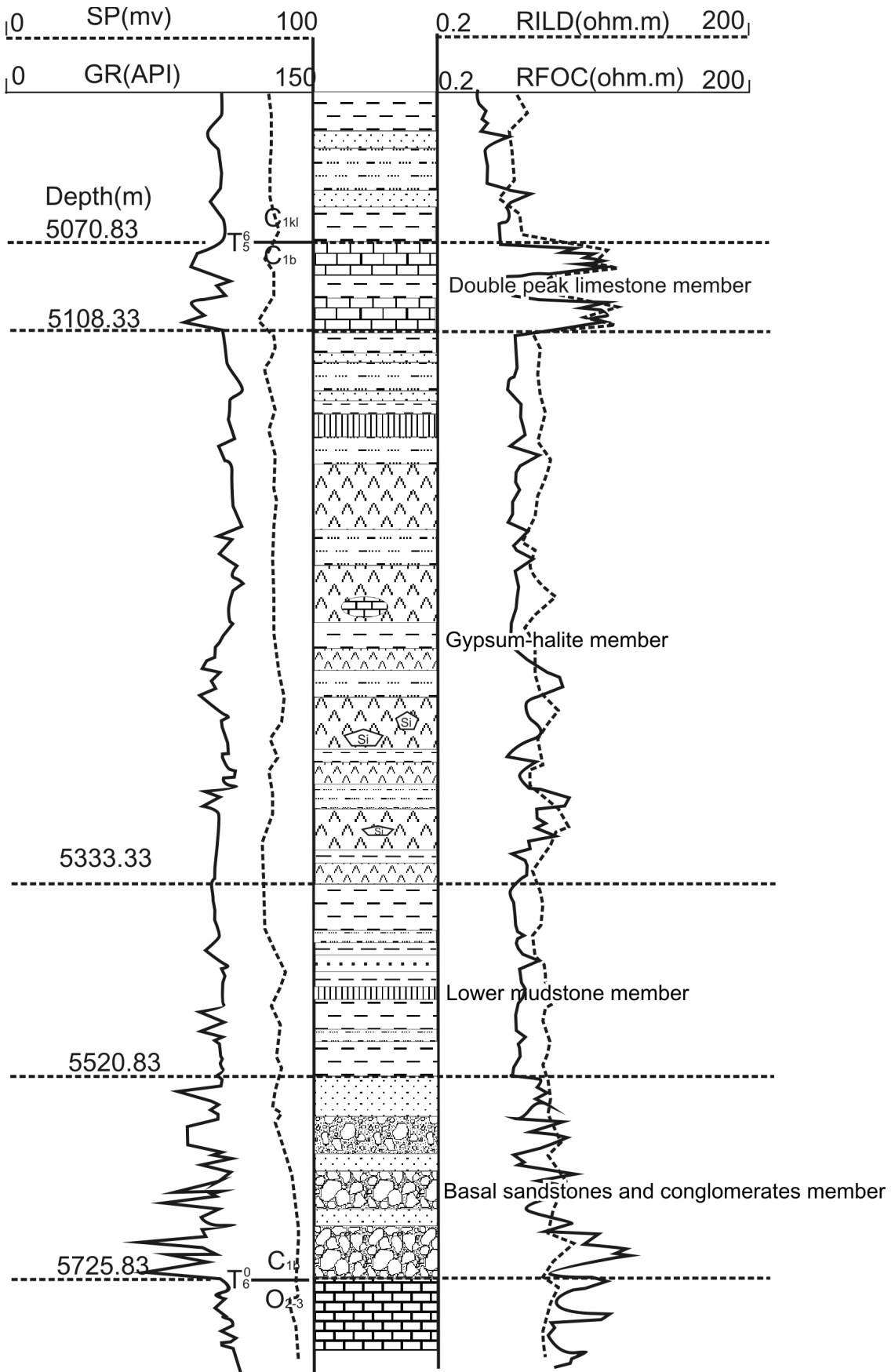


Fig. 4. Lithostratigraphy of the Lower Carboniferous Bachu Formation at well S10, northern Tarim Basin (see Fig.1 for well location). The so-called “Double-Peak Limestone Member” is clearly identifiable on the log traces. Note that GR and RFOC response characteristically decrease upwards through the formation.

Fig. 5a-e. Typical 2D and 3D seismic sections across the studied saltbody.

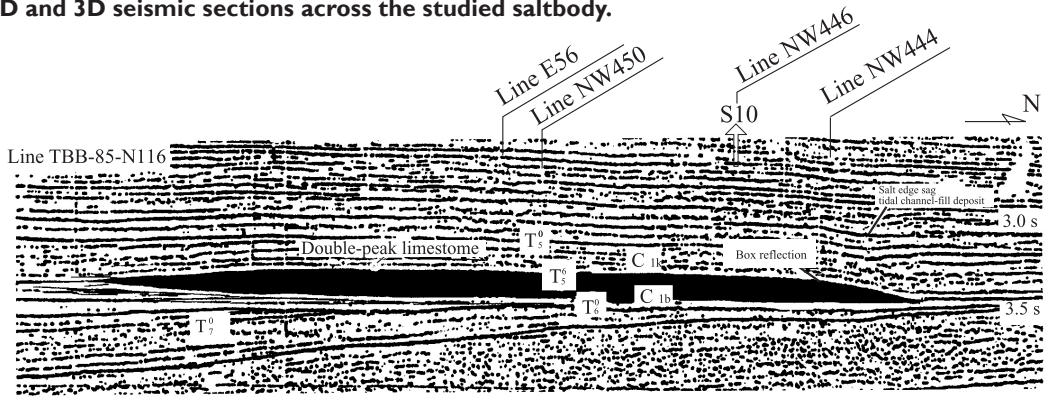


Fig.5a Line TBB-85-N116 (see Fig.1 for location).

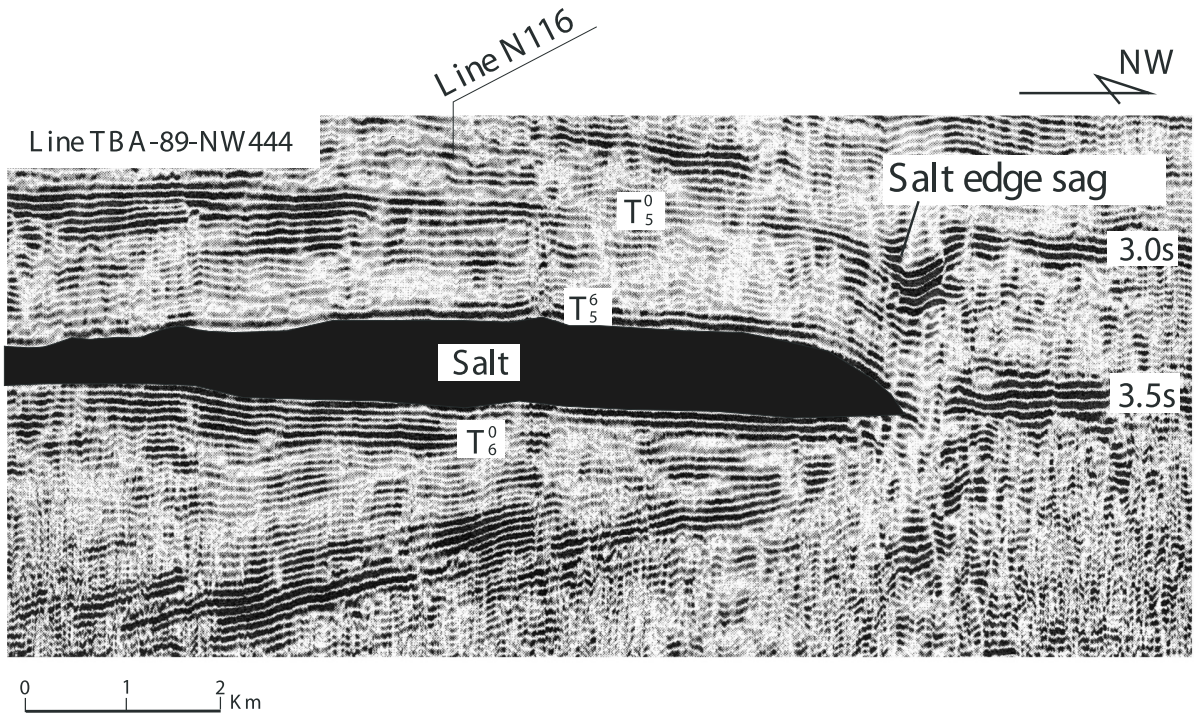


Fig. 5b. Seismic line TBA-89-NW444 (see Fig.1 for location).

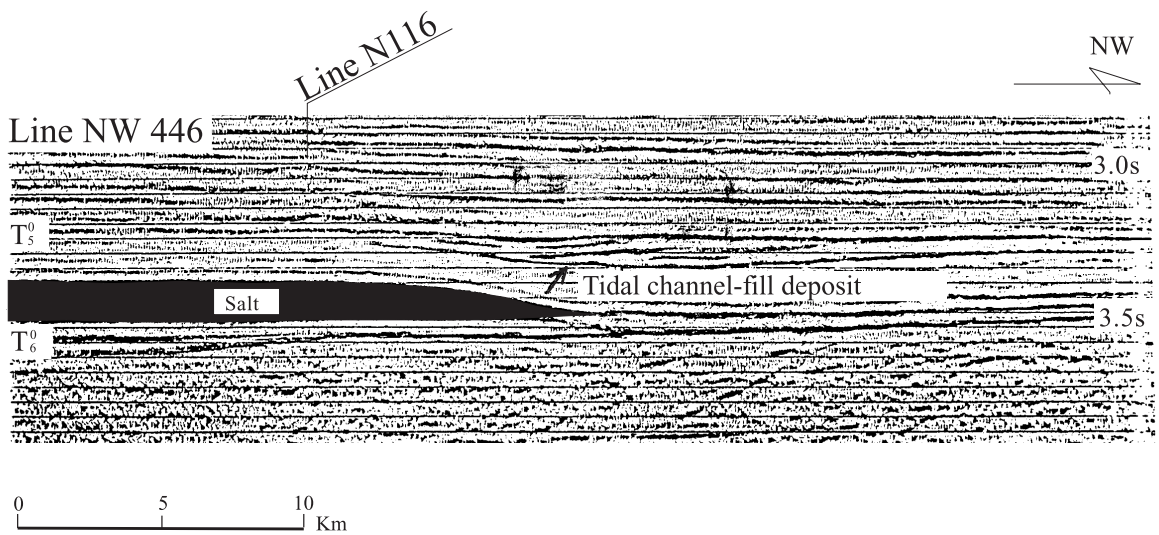


Fig. 5c. Seismic line NW446 (see Fig.1 for location).

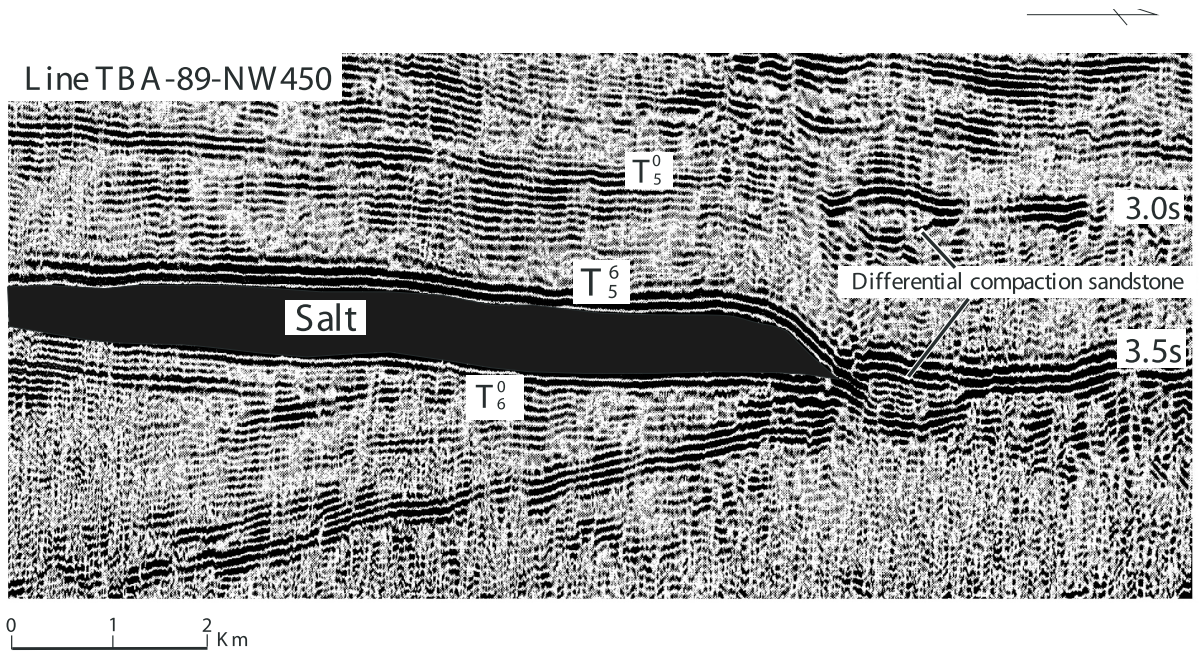


Fig. 5d. Seismic line NW450 (see Fig.1 for location).

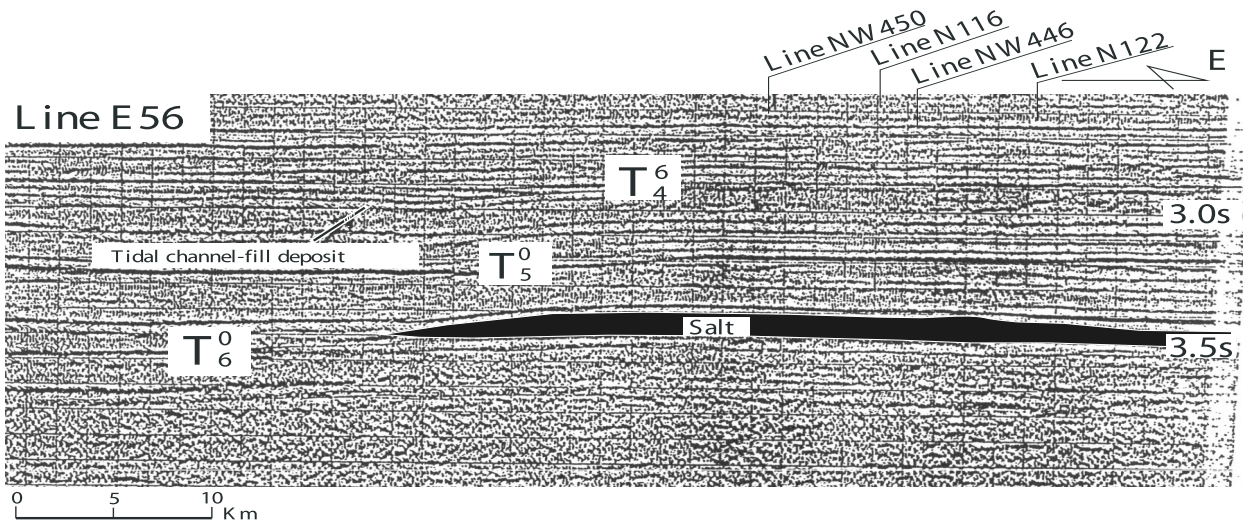


Fig. 5e. Seismic line E56 (see Fig.1 for location).

sandstones. The lenticular form of some of the sandbodies may be due to possible late-stage differential compaction. The formation and location of the sag belts reflects the history of salt deformation and withdrawal. The clastic deposits in the sags can be dated approximately by correlating seismic horizons, and also from stratigraphic data from the wells (Gu, 1996; Kang, 1996; Zhou *et al.*, 1999). Thus we were able to reconstruct the deformation history of the salt in the study area, and three phases of plastic movement were tentatively identified:

1. The first phase occurred at the end of the Early Permian. This coincided with regional tectonism associated with the collision of the NE Junggar block, and the northward subduction of SW palaeo-Tethys beneath the Tarim block. This was accompanied by the formation of the Tianshan fold-belt and inferred north- and SWward regional extrusion with uplift in the northern Tarim Basin (Zhu, 1989; Jia *et al.*, 2002; Yang *et al.*, 2002; Gu, 1996; Xinjiang BGMR, 1993). Material depletion induced by salt migration resulted in the collapse of Carboniferous strata to form peripheral sags round the saltbody margins.

2. A second phase of salt migration occurred at the end of the Triassic (possibly extending locally to the earliest Jurassic). This is related to SWward regional extrusion induced by collision between the Qiangtang and Tarim blocks with continued northward subduction of palaeo-Tethys (Zhu, 1989; Jia *et al.*, 2002; Xinjiang BGMR, 1993; Yang *et al.*, 2002). Salt migration resulted in the collapse of Triassic - Lower Jurassic strata and the formation of a second marginal depression belt around the saltbody. On seismic sections (Fig. 5), the channel-fill deposits appear to have a foresetted internal structure. The depressions were the sites of lateral channel accretion in the direction of salt migration (Fig. 7 a, b and c).

3. The third phase of salt movement occurred at the end of the Late Tertiary and was associated with the India—Eurasia collision and intense subsidence of the Kuche depression in northern Tarim (Xinjiang BGMR 1993; Jia *et al.*, 2002), and the formation of the Kuche foreland basin and thrust belt in front of the Tianshan foldbelt (Fig. 1). Regional dips changed from southward to northward (Zhu, 1989; Jia, 1999, 2002; Yang *et al.*, 2002). The northern margin of the saltbody flowed northwards possible due to gravitational effects, and the western margin was displaced eastwards (Fig. 6). This phase of salt migration resulted in the formation of a series of small-scale normal faults, together with some low-amplitude salt-edge and salt-dome anticlines.

Direction and Distance of Salt Migration

The extent of saltbody migration can be estimated by considering the width of the marginal troughs

associated with the various episodes of salt withdrawal. The general methodology used is shown schematically in Fig. 8. Firstly, the pinch-out points of the salt (L_0 , L_1 , L_2) were located; then the lengths L_0 - L_1 and L_1 - L_2 were measured; and finally the horizontal distance of salt flow (i.e. one-half of L_0 - L_1 and L_1 - L_2) was determined.

The results show that salt migration at the end of the Early Permian was characterized by some 2.0-2.8km southwards withdrawal of the northern margin of the saltbody, and approximately 2.0km eastwards withdrawal of the western margin (Fig. 6). Conversely, at the end of the Early Jurassic, the western margin migrated a greater distance eastwards (2.0-2.5km) than the northern margin (1.0-1.8km southwards); and the NE margin migrated NEwards by 1.0km. At the end of the Tertiary, the salt flowed northwards by about 0.6-1.5km; while at the western margin, the salt flowed eastwards by 0.4-0.5km.

PLASTIC SALT FLOW AND TRAP FORMATION

Structural traps associated with salt flow are recognized as important exploration targets (Jenyon, 1986; Jackson *et al.*, 1995; Mello *et al.*, 1994). Salt-related structures in eastern China have been investigated by Chinese explorationists; examples include the Dongpu Depression, Bohai Bay Basin, Subei Basin and Jiangnan Basin (Zhu, 1989; Wang *et al.*, 1990).

Sag belts on the margins of Carboniferous saltbodies in the northern Tarim Basin have been targeted in recent years leading to the discovery of the *Shantamu*, *Aixieke* and *Daliya* oil- and gasfields (Kang, 1986) (locations in Fig. 1).

Salt movement and overburden faulting

Salt movement commonly causes faulting in the overburden (Jenyon, 1986; Nelson, 1991; Koyi *et al.*, 1993; Rowan *et al.*, 1999). Physical modelling has shown that small-scale faults and thrust can occur in the overburden near to, or at the sides of, segmented secondary salt sheets (Wu *et al.*, 1990a and b; Seni, 1992; Koyi, 1996; Ge *et al.*, 1997).

In the study area, a number of small-scale normal faults and thrusts occur locally in the overburden above the marginal sag belt and are interpreted to result from salt migration. No relationship with deeper-lying basement faults was observed (Fig. 7d, e and f). The marginal and suprasalt normal faults and thrusts cut through Carboniferous, Triassic and Early Jurassic strata.

Marginal normal faults are generally due to gravitational collapse of marginal salt sags, and have vertical displacements of 40 to 80m. Suprasalt normal

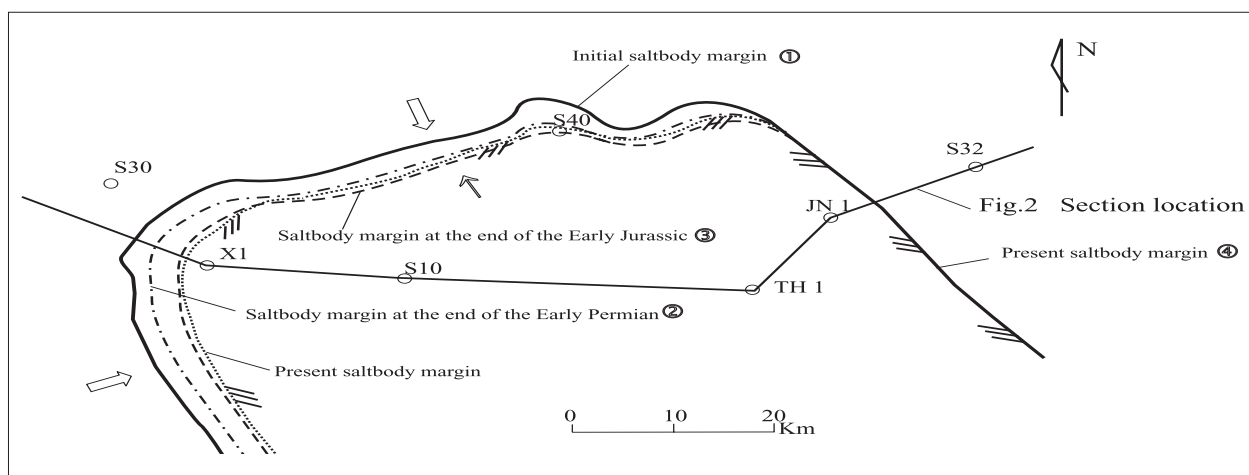


Fig. 6. Schematic map showing the plan-view deformation of the Carboniferous saltbody.

faults and thrusts had vertical displacements of about 20-60m. Marginal normal faults may constitute important pathways for oil and gas migration in the study area.

Salt-related structural traps

Structural traps in the study area related to salt flow include salt ridge anticlines, domal anticlines and marginal troughs (Figs. 9 and 10).

Salt ridge anticlines frequently occur above the margins of the saltbody, and are interpreted to be due to thickening of the salt interval as a result of lateral migration. Small-scale salt ridge anticlines have been identified in suprasalt Triassic strata (Fig. 9 and 10) and have a mean amplitude of about 13m with a closure area of about 4sq. km. Numerous normal faults parallel to the margin of the salt sheet occur in the overburden around these features, and may constitute effective migration routes for oil and gas.

Larger-scale *domal anticlines* occur in suprasalt Carboniferous and Triassic strata due to asymmetric lateral salt flow and form good exploration targets (Figs. 9 and 10). These features have amplitudes of about 26m with closure areas of around 15sq. km. However, they are seldom associated with faulting.

Marginal troughs or sags frequently form due to lateral salt withdrawal, and are generally filled by channel bodies whose lenticular geometry and foresetted internal structure can often clearly be identified in seismic sections. Lateral channel accretion appears to occur in the same direction as salt withdrawal (Fig. 7a,b, c, and Fig.10). On seismic sections, we estimate that the widths of two such marginal troughs are around 0.5-1.0km and 0.2-0.5km, respectively.

In our study area, seven types of condensate, oil and gas plays have been discovered. The *Aixieke*, *Shantamu*, and *South Aixieke* fields (for locations, see Fig. 1) have been found in supra-salt traps related to

salt flow; others are associated with supra- and subsalt stratigraphic traps (Fig.1, Fig. 9). They occur respectively in the basal and upper sandstone member of the Kalashayi Formation (Lower Carboniferous); the lower and upper sandstone member of the middle Triassic; and in upper Triassic sandstones.

In the first type, sag-belt fill sandstones (latest Carboniferous -- earliest Triassic), which may have been deformed as a result of differential compaction, host oil- and gas in a marginal trough extending along the east-west margin of the salt sheet. The other two comprise a salt ridge (Triassic) and a salt dome (Middle-Upper Triassic and Lower Jurassic), respectively.

REASONS FOR THE ABSENCE OF SALT DIAPIRS

Growth of salt diapirs generally begins at depths of around 1,800m in response to inverse density gradients between the salt and the overburden (Wilson, 1993; Jackson, 1995; Ge *et al.*, 1997; Montgomery *et al.*, 1997). Lower Carboniferous salt in the study area is buried to more than 5,000m. However no salt diapirs have been identified and this could be for the following reasons:

1. The salt interval in the study area is only 115-225m thick and this thickness may not be adequate for the initiation of diapiric growth which is often associated with much thicker (1,000m or more than 2000m) salt intervals (Jenyon *et al.*, 1986, 1988; Jackson, 1995).
2. Experimental and field examples have drawn attention to the influence of sub-salt basement faults and regional extension to diapir initiation and growth (Koyi *et al.*, 1993; Jackson *et al.*, 1994; Rowan, 1995; Rowan *et al.*, 1995; Schultz-Ela *et al.*, 1996). However, the northern Tarim Basin has been influenced by regional

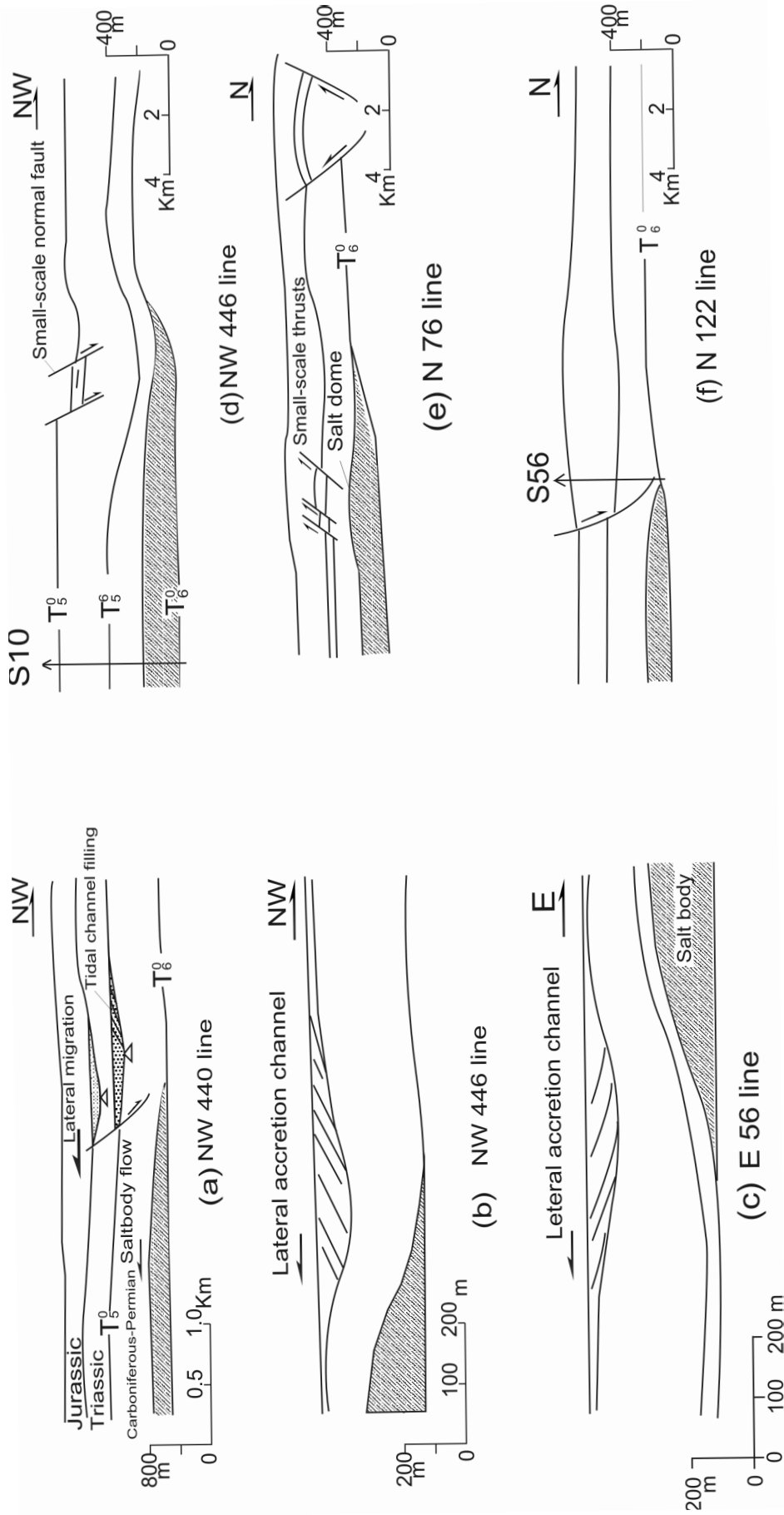


Fig.7. Structural features associated with the margins of deforming salt sheets:
 (a) Superposed lateral migration of salt-margin channel.
 (b) and (c). Lateral accretion of channel fill in the direction of salt flow.
 (d) Small-scale normal faults in overburden of sag belt.
 (e) Small-scale thrust in overburden of salt dome.
 (f) Small-scale normal faults at saltbody margin.

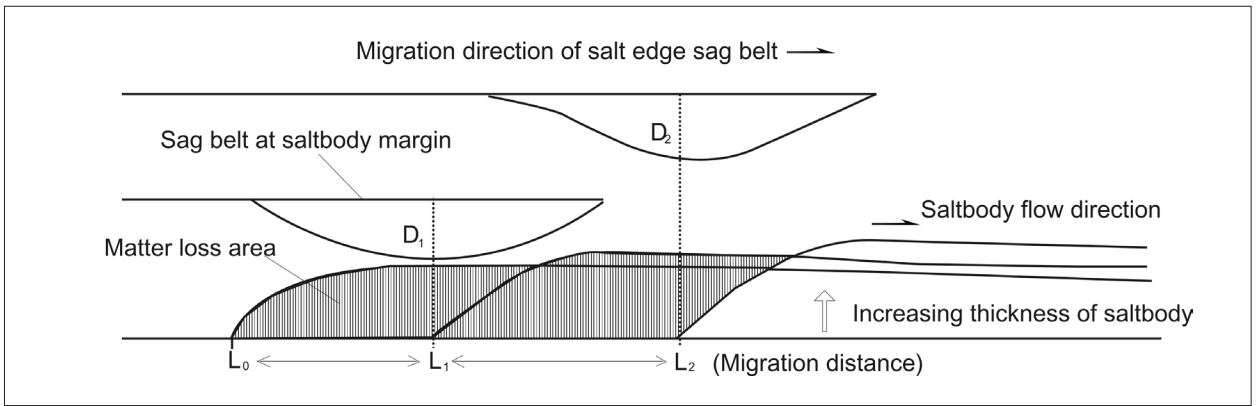


Fig. 8. Ideal model of the relationship between plastic salt flow and a marginal sag belt. D_1 and D_2 represent the axes of successive troughs; these correlate with the successive locations of the margins of the saltbody (L_1 and L_2) as material is withdrawn to the right of the panel. The half-width (L_1-L_2) of the marginal trough is equal to the horizontal distance of salt withdrawal.

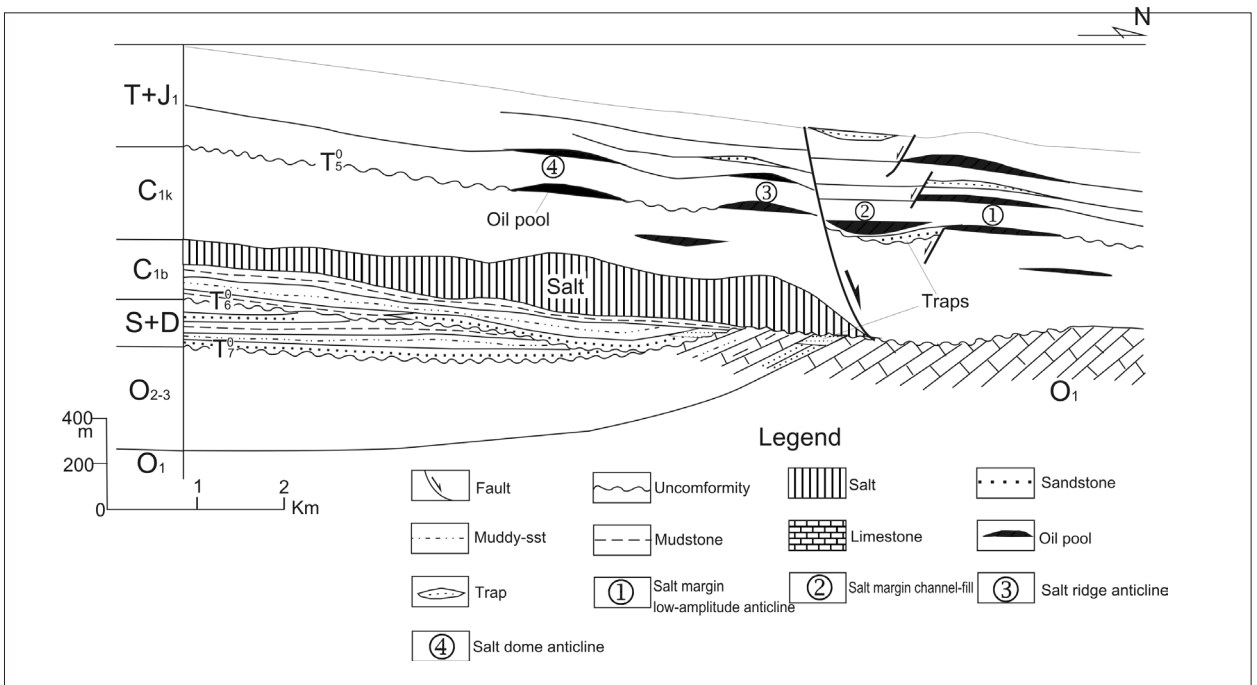


Fig. 9. Types and distribution of potential traps and oil pools related to salt flow in the Akekule area in the northern Tarim Basin

extrusion during Late Permian to Tertiary times with little extension; and no basement fault have been reported in the study area.

3. The saltbody is buried to more than 5,000m and the overburden pressure is around 130-140MPa, which is greater than the buoyancy force exerted by the salt interval itself. This may explain why the salt has undergone lateral flow but not upward flow in the form of a diapir.

CONTROLS ON SALT FLOW

Previous studies on the mechanisms of plastic salt flow and deformation include Jenyon *et al.*, 1988; Jackson, 1995; West, 1989; Koyi, 1996; Rowan, 1993, 1995;

Talbot *et al.*, 1996; Guglielmo *et al.*, 1997; Ge *et al.*, 1997; and McBride *et al.*, 1998. The principal factors which may have controlled salt deformation in the study area are temperature, stress and fluid composition. These factors are considered in turn below:

Temperature

The influence of temperature on the creep rate of halite has been demonstrated by many researchers (LeComte, 1965; O'Brien *et al.*, 1984,1988; Jenyon, 1986). For example, Jenyon (1986) noted that halite samples showed a rapid acceleration in creep rate when they were heated to about 423K. These studies

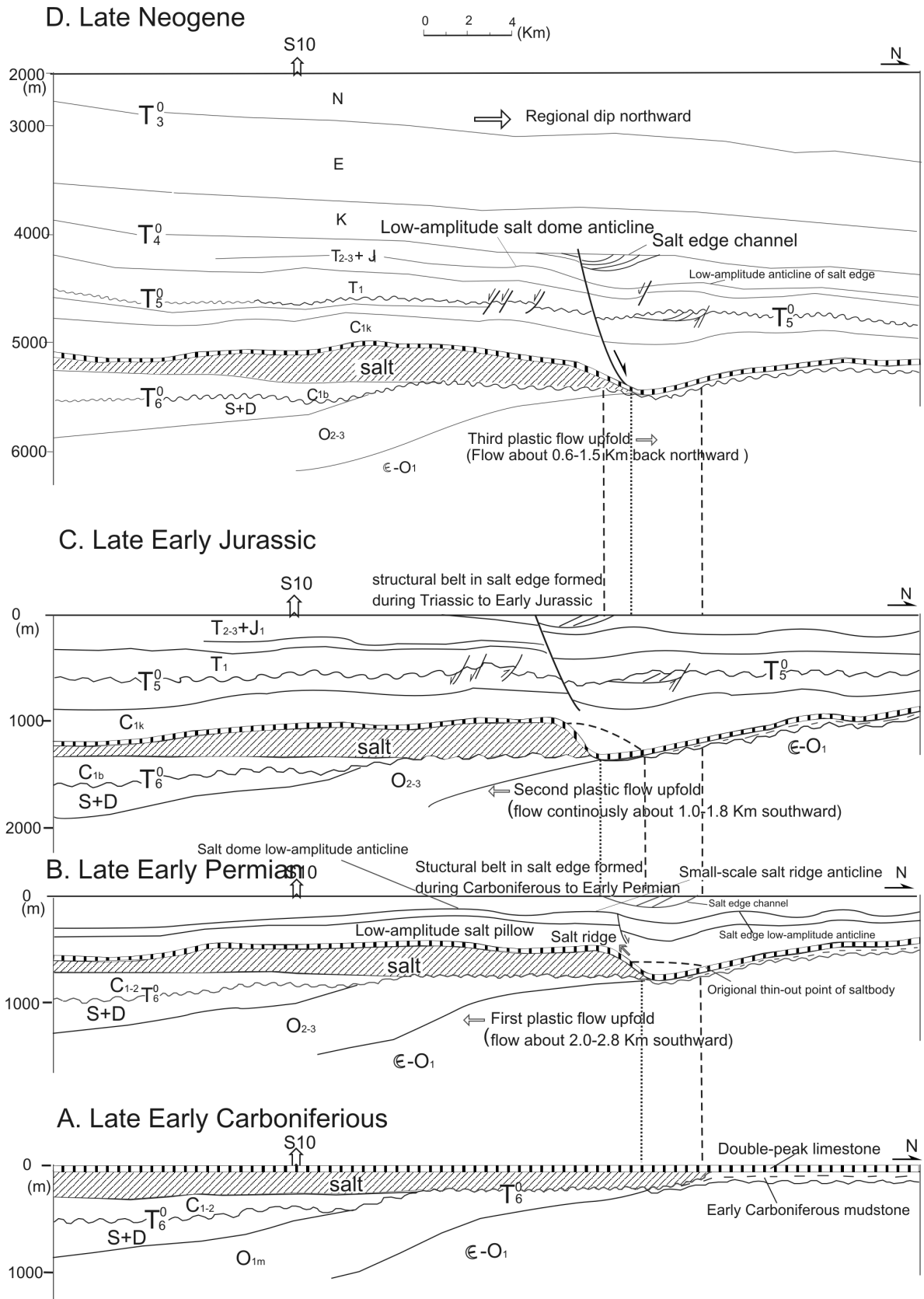


Fig. 10. Summary diagrams illustrating the development and deformation of Lower Carboniferous saltbodies in the northern Tarim Basin.

show that salt will begin to flow easily at temperature above 100°C.

The average palaeo-geothermal gradient in the northern Tarim Basin was 2.4 °C/100m during the Palaeozoic, 2.0-2.2 °C/100m during the Mesozoic and Cenozoic, and is 1.7-2.4 °C/100m at the present day (Jia, 1991; Kang, 1996). We calculate that the highest palaeo-temperatures to which the Lower Carboniferous saltbody in the study area was exposed were 120-130°C, which should be sufficient to allow plastic movement.

Stress history (Fig. 10)

The first phase of large-scale plastic salt flow occurred at the end of the Early Permian due to north-south and SW-NE compression (Fig.10A-B) (*see above*). During the Late Permian late Hercynian orogenic phase, block faulting in the northern Akekule region occurred together with plastic flow of Lower Carboniferous salt to the south. The block faulting reactivated pre-existing east-west-trending thrusts in the Akekule area (Jia, 1991; Kang, 1996; Jia *et al.*, 2002). Salt migration resulted in the formation of low-amplitude compressional anticlines, domes and marginal troughs which are associated with normal faults.

Less intense regional compression affected the northern Tarim area during the Late Triassic–Earliest Jurassic Indosinian orogenic phase and the Early Jurassic-Late Cretaceous Yanshanian orogeny, with minor thrusting and folding associated with fault reactivation (Jia *et al.*, 2002). Regional uplift of the northern Tarim Basin occurred during the Yanshanian episode (Jia, 1999; Kang, 1996).

Indosinian and Yanshanian tectonism, with SW-NE oriented compression and subsidence of the northern part of the basin, resulted in a second phase of plastic flow of Lower Carboniferous salt, giving rise to low-amplitude salt ridges and marginal troughs (Fig.10C). Intense SW-NE compression in the Late Hercynian reworked east-west trending anticlines and salt domes, whose axes changed from NW to SE trending. Because the western margin of the saltbody was under compression, eastward plastic flow occurred and formed the convex arc-shaped margin of the saltbody to the NW.

During the Late Tertiary Himalayan orogenic phase, the northern Tarim Basin subsided due to flexural loading as a result of the south-verging foldbelt to the north. In response, regional dips changed from south to north (Jia, 1991; Jia, 1999). The Lower Carboniferous saltbody may have undergone a third, north-directed phase of gravity-driven plastic flow in the Late Tertiary, accompanied by eastwards migration of its western margin (Fig. 10D).

Stress field modelling using the 3D finite element method (Wang *et al.*, 1999) also show that the magnitude of the principal compressional stress was 80-130 MPa between the late Hercynian and the present-day. This greatly exceeds the threshold of salt flow (14MPa) (Jenyon *et al.*, 1986,1988; Jackson *et al.*, 1995), and also that of superjacent strata (30-40MPa) during the Hercynian and Indosinian orogenies (Kang, 1996; Wang *et al.*, 1999). The stress difference resulted in lateral flow and uplift of the plastic salt sheet, and the rapid increase of the saltbody's thickness at the margins.

The change of marginal configuration and the lateral migration of the saltbody may indicate that the compression stress from the north in the late Hercynian was greater than that from the SW; conversely, during the Indosinian, stresses from the SW were greater than those from the north (Fig. 6).

Fluid Composition

Widespread and rapid dissolution of salt takes place when it is exposed to an undersaturated solution of NaCl in conditions of elevated stress (Jenyon, 1986). The chemical composition of formation waters from the Lower Carboniferous Bachu Formation at seven wells was analysed using ion chromatography (Laboratory of Chemical Analysis, Northwest Bureau of Petroleum Geology, CINOPEC, Urumqi, China), and results are shown in Table 3. They show that palaeofluids in the study area are rich in sodium (Na is 79,590 mg/L on average) and chlorine (Cl is 101,920 mg/L on average). In the east of the salt body, formation waters are relatively enriched in Ca²⁺, HCO₃ and CO₂ but show reduced Na and Cl contents, reflecting the fluids' origin from basinal areas to the east (Zhou *et al.*, 1999) (Table 3). The restricted relationship between clastic rock and salt and reduced dissolution may explain why little plastic salt flow took place at the east margin of the saltbody (Fig. 6).

CONCLUSIONS

1. Structural traps associated with the migration of Lower Carboniferous salt in the northern Tarim Basin comprise salt ridge anticlines, domal anticlines, and marginal troughs or synclines. Salt-ridge and salt edge low-amplitude anticline are the most important oil and gas exploration targets.

2. Three episodes of salt flow have been recognized and each may be related to a phase of regional compression during, respectively, the Late Hercynian (Early Permian), Indosinian (Late Triassic and Earliest Jurassic) and Himalayan (end-Tertiary) orogenic phases. During each episode, the direction and extent of salt migration varied at the margins of the saltbody.

Wells	Depth (m)	Relative density of formation water (g/cm^3)	Ion content (mg/L)								Mineralization (mg/L)
			Na^+	K^+	Mg^{2+}	Ca^{2+}	Cl^-	SO_4^{2-}	HCO_3^-	CO_3^{2-}	
S30	5350	1.279	102634	4567	378.7	9804	125643	2078.2	267.45	131.45	205643
S40	5270	1.1876	113587	3875	367.2	8756	136754	1897.4	236.87	129.65	216547
XI	5230	1.0753	107654	4768	447.9	9903	99656	2033.4	187.98	138.67	157795
S10	5200	1.0332	113455	3568	689.3	10567	55206	2107.7	195.5	127.06	205463
THI	5320	1.2354	108374	3589	367.4	8854	51986	2637.1	234.78	187.98	198645
JNI	5300	1.2036	6549	3147	287.9	12510	127689	1807.8	307.67	206.4	96754
S32	5250	1.1653	4876	3653	467.4	11768	116506	1654.2	289.5	216.76	84352
<i>Average</i>		<i>1.1685</i>	<i>79590</i>	<i>3881</i>	<i>429.4</i>	<i>10309</i>	<i>101920</i>	<i>2030.8</i>	<i>245.68</i>	<i>162.57</i>	<i>166457</i>

Table 3. Chemical composition of Lower Carboniferous formation waters (Bachu Formation, C1b) from the salt-bearing interval at wells in the northern Tarim Basin.

3. The main factors affecting salt deformation were temperature, stress and fluid composition, of which stress is the most important in the northern Tarim Basin.

4. Vertical salt diapirs are not present in the study area and this may reflect (i) the relatively small thickness of the Carboniferous salt interval; (ii) the absence of sub-salt (basement) faults; (iii) the absence of a significant episode of regional extension during the basin's development.

ACKNOWLEDGEMENTS

This study was financially supported by the Programming Institute of the Northwestern Bureau of Petroleum Geology, CINOPEC, Urumqi. We thank Hemin Koyi, Martin Jackson, and Mark Rowan for helpful reviews of the manuscript; two anonymous referees also provided valuable comments.

REFERENCES

- GE, H. X., JACKSON, M. P.A. and VENDEVILLE, B. C., 1997. Kinematics and dynamics of salt tectonics driven by progradation. *AAPG Bull.*, **81**(3), 398-423.
- GE, H. X., JACKSON, M. P.A. and VENDEVILLE, B. C., 1997. Structure evolution of the Wenliu salt diapir and graben, Bohai Bay. *Acta Petrolei Sinica*, **18**(2), 35-40.
- GRAHAM, S.A., XIAO, X., CARROLL, A.R., et al., 1990. Characteristics of selected petroleum-source rocks, Xinjiang Uygur Autonomous Region, northwest China. *AAPG Bull.*, **74**(4), 493-512.
- GU, J.Y., (Ed.), 1996. Depositional sequences and evolution of the Tarim Basin. Beijing: Petroleum Industry Press.
- GUGLIELMO, Jr. G., JACKSON, M. P.A. and VENDEVILLE, B. C., 1997. Three-dimensional visualization of salt walls and associated fault system. *AAPG Bull.*, **81**(1), 46-61.
- JACKSON, M. P.A. and TALBOT, C. J., 1989. Salt canopies. In: Gulf of Mexico salt tectonics, associated processes and exploration potential: Gulf Coast Section SEPM Foundation 10th Annual Research Conference, Houston, Texas, 72-78.
- JACKSON, M. P.A. and VENDEVILLE, B. C. 1994. Regional extension as a geologic trigger for diapirism. *Geological Society of America Bulletin*. **106**, 57-73.
- JACKSON, M.P.A., 1995. Retrospective salt tectonics. In: M. P. A. Jackson, D. G. Roberts and S. Snelson (Eds), Salt tectonics: a global perspective. *AAPG Memoir* **65**, 1-28.
- JENYON, M.K., 1986. Salt tectonics. Elsevier, London and New York.
- JENYON, M. K., 1988. Some deformation effects in a clastic overburden resulting from salt mobility. *Journ. Petrol. Geol.*, **11**(3), 66-77.
- JIA, C. Z. 1999. Structural characteristics and oil-gas accumulative regularity in the Tarim Basin. *Xinjiang Petroleum Geology*, **20**(3), 177-183.
- JIA, C.Z. and WEI G.Q. 2002. Structural characteristics and petroliferous features of Tarim Basin. *Chinese Science Bulletin* **47**, 1-11.
- JIA, R.X. (Ed.), 1991. Study of oil-gas geology in northern Tarim Basin, China (Vol. 1). Wuhan: China University of Geosciences Press.
- KANG, Y. Z., (Ed.), 1996. Petroleum geology and resource assessment in the Tarim Basin, Xinjiang, China, Beijing: Geological Publishing House, 1-140, 244-240.
- KOYI, H. 1992. Modeling of segmentation and emplacement of salt sheets. *Geological Society of America*, Abstracts with Programs, A363.
- KOYI, H. 1996. Salt flow by aggrading and prograding overburdens. In: Alsop, G. I., Blundell, D. J. and Davison, I. (Eds.), *Salt Tectonics. Geol. Soc. Spec. Publ.* **100**, 243-258.
- KOYI, H. and PETERSEN, K., 1993. The influence of basement faults on the development of salt structures in the Danish basin. *Marine and Petroleum Geology*, **10**(2), 82-94.
- KOYI, H., JENYON, M.K. and PETERSEN, K. 1993. The effect of basement faulting on diapirism. *Journal of Petroleum Geology*, **16**, 285-312.
- LECOMTE, P., 1965. Creep in rock salt. *Journal of Geology*, **73**, 469-484.
- LETOUZEY, J., COLLETTA, B., VIALLY, R., and CHERMETTE, J.C., 1995. Evolution of salt-related in compressional settings. In: M. P.A. Jackson, D. G. Roberts, and S. Snelson (Eds), Salt tectonics: a global perspective. *AAPG Memoir* **65**, 41-60.
- LIU DAMENG, TU JIANQI and JIN KUILI, 2003. Organic petrology of potential source rocks in the Tarim Basin, NW China. *Journ. Petrol. Geol.*, **26**(1), 105-124.
- McBRIDE, B. C., ROWAN, M.G. and WEIMER, P., 1998. The evolution of allochthonous salt systems, northern Green Canyon and Ewing Bank (offshore Louisiana), northern Gulf of Mexico. *AAPG Bulletin*, **82**(5B), 1013-1036.
- MELLO, U. T., ANDERSON, R.N. and KARNER, G. D., 1994. Salt restrains maturation in subsalt plays. *Oil & Gas Journal*, **92**(5), 101-108.
- MONTGOMERY, S. L. and ERICKSON, R. L., 1997. Dry creek salt dome, Mississippi interior salt basin. *AAPG Bull.*, **81**(3), 351-366.
- MONTGOMERY, S. L. and MOORE, D. "C.", 1997. Subsalt play, Gulf of Mexico: A review. *AAPG Bull.*, **81**(6), 871-896.
- NELSON, T. H., 1991. Salt tectonics and listric normal faulting. In: Salvador, A. (Ed.), *The Geology of North America, The Gulf of Mexico Basin*, Geological Society of America, 73-89.
- O'BRIEN, J. J. and I. LERCHE, 1984. The influence of salt domes on paleotemperature distributions. *Geophysics*, **49**, 2032-2043.
- O'BRIEN, J. J. and I. LERCHE, 1988. Impact of heat flux anomalies around salt diapirs and salt sheets in the Gulf Coast on hydrocarbon maturity. *Gulf Coast Ass. Geol. Soc.*, **58**, 231-243.
- ROWAN, M. G., 1995. Structural styles and evolution of allochthonous salt, central Louisiana outer shelf and upper slope. In: M. P. A. Jackson, D. G. Roberts and S. Snelson (Eds), Salt tectonics: a global perspective. *AAPG Memoir* **65**, 199-228.
- ROWAN, M. G., McBRIDE, B. and WEIMER, P., 1995. The role of extension in the evolution of allochthonous salt, central Louisiana outer shelf and upper slope. In: C. J. Travis, H. Harrison, M. R. Hudec et al., (Eds), Salt sediment and hydrocarbons. Gulf Coast Section SEPM Foundation 16th Annual Research Conference, Houston, Texas, 223-231.
- ROWAN, M.G., 1993. A systematic technique for the sequential restoration of salt structures. *Tectonophysics*, **228**, 331-348.
- ROWAN, M.G., JACKSON, M.P.A. and TRUDGILL, B.D., 1999. Salt-Related Fault Families and Fault Welds in the Northern Gulf of Mexico. *AAPG Bulletin*, **83**(9), 1454-1484.
- SCHULTZ-ELA, D. D. and JACKSON, M. P.A., 1996. Relation of subsalt structures to suprasalt structures during extension. *AAPG Bulletin*, **80**(12), 1896-1924.
- SENI, S. J., 1992. Evolution of salt structures during burial of salt sheets on the slope, northern Gulf of Mexico. *Marine and Petroleum Geology*, **9**, 452-468.
- TALBOT, C. J., 1992. Centrifuged models of Gulf of Mexico profile. *Marine and Petroleum Geology*, **9**, 452-468.
- WANG, X. P., QI, F. and ZHANG, J. H. (Eds), 1990. Tectonic analysis of petroleum exploration. Wuhan: China University of Geosciences Press.
- WANG, X. S., SONG, H. Z. and LIU, J., 1999. Numerical

- modeling of tectonic stress field in Tarim Basin and its implication to hydrocarbon accumulation. *Seismology and Geology*, **3**, 268-274.
- WEST, D. B. 1989. Model for salt deformation on deep margin of central Gulf of Mexico basin. *AAPG Bull.*, **73**, 1472-1482.
- WILSON, H. H., 1993. The age of salt in the Gulf of Mexico basin. *Journal of Petroleum Geology*, **16**, 125-152.
- WU, S., BALLY, A. W. and CRAMEZ, C. 1990a. Allochthonous salt, structure and stratigraphy of the north-eastern Gulf of Mexico. Part 1: Structure. *Marine and Petroleum Geology*, **7**, 318-333.
- WU, S., VAIL, P. R. and CRAMEZ, C. 1990b. Allochthonous salt, structure and stratigraphy of the north-eastern Gulf of Mexico. Part 2: Stratigraphy. *Marine and Petroleum Geology*, **7**, 334-370.
- XINJIANG BGMR [Bureau of Geology and Mineral Resources of Xinjiang Uygur Autonomous Region], 1993. Regional geology of Xinjiang Uygur Autonomous Region, Geological Memoirs, Series 1, Number 32: Beijing, Geological Publishing House, pp. 657-759.
- YANG S., JIA C., CHEN H., WEI, G., et al., 2002. Tectonic evolution of Tethyan tectonic field, formation of northern margin basin and explorative perspective of natural gas in Tarim basin. *Chinese Science Bulletin* **47**, 34-41.
- ZHOU, J. Y., HAN, Y. Y. and LIN, Z. M., 1999. Sedimentary evolution and salt-forming mechanism in Lower Carboniferous salt-bearing series, northern Tarim Basin. *Xinjiang Petroleum Geology*, **20**(3), 244-247.
- ZHU, X. 1989. Chinese Sedimentary Basins. In: K. J. Hsu (Ed.), *Sedimentary Basins of the World*. Elsevier, pp 33-44 and 207-228.
-